



TITLE:

# Numerical Stability Analysis of Space-Time Finite Integration Method Based on the Dependent Domain Concept

AUTHOR(S):

Katsuki, Keinoshin; Asahino, Shogo; Mifune, Takeshi; Matsuo, Tetsuji

---

CITATION:

Katsuki, Keinoshin ...[et al]. Numerical Stability Analysis of Space-Time Finite Integration Method Based on the Dependent Domain Concept. IEEE Transactions on Magnetics 2022, 58(9): 7200304.

ISSUE DATE:

2022-09

URL:

<http://hdl.handle.net/2433/276142>

RIGHT:

© 2022 IEEE. Personal use of this material is permitted. Permission from IEEE must be obtained for all other uses, in any current or future media, including reprinting/republishing this material for advertising or promotional purposes, creating new collective works, for resale or redistribution to servers or lists, or reuse of any copyrighted component of this work in other works.; This is not the published version. Please cite only the published version. この論文は出版社版ではありません。引用の際には出版社版をご確認ください。

# Numerical Stability Analysis of Space-Time Finite Integration Method Based on the Dependent Domain Concept

Keinoshin Katsuki<sup>1</sup>, Shogo Asahino<sup>1</sup>, Takeshi Mifune<sup>1</sup>, and Tetsuji Matsuo<sup>1</sup>

<sup>1</sup>Graduate School of Engineering, Kyoto University, Kyoto, 615-8246 Japan, katsuki.keinoshin.33u@st.kyoto-u.ac.jp

**A method for estimating the stability criterion in the space-time finite integration method using the subgrid technique was developed. Numerical and analytical dependent domains were compared to estimate the stability limit. Space-time subgrids locally refined with two, three, and four divisions were examined. The stability limit based on the proposed method almost agrees with that of the numerical experiment.**

*Index Terms*—Dependent domain, finite integration method, numerical stability, space-time grid

## I. INTRODUCTION

**A**N EFFICIENT method for electromagnetic wave computation is required in the analysis of advanced optical device materials such as metamaterials and photonic crystals, which locally have fine structures at sub-wavelength scales. For the analysis of these devices, the application of the subgrid technique [1] to the conventional finite difference time domain (FDTD) method often causes numerical instability unless sophisticated stabilization is implemented, whereas the finite integration (FI) method [2][3][4] can simulate wave propagation efficiently using flexible spatial grids. However, its time step is restricted by the Courant–Friedrichs–Lewy (CFL) condition [5], depending on the smallest spatial grid size.

As an expansion of the FI method, the space-time FI [6] method was developed, where the primal and its dual grid were constructed in space-time. This method reduces the computational cost of handling local microstructures by flexibly configuring both the spatial and the temporal grids. It has been observed that the space-time FI method with the subgrid technique is conditionally stable when using an explicit time-marching scheme [7]. However, the stability limit must be obtained experimentally by numerical examination. This study proposes a method to estimate the stability limit from the space-time grid geometry based on the dependent domain concept [5], which in turn is based on the inclusion relationship between the numerical dependent and analytical dependent domains.

## II. SPACE-TIME FINITE INTEGRATION METHOD

The coordinate system is denoted by  $(ct, x, y, z) = (x^0, x^1, x^2, x^3)$ , where  $c = 1/\sqrt{\varepsilon_0\mu_0}$  and  $\varepsilon_0$  and  $\mu_0$  are the permittivity and permeability of the vacuum, respectively. The Maxwell equations are written in integral form as

$$\oint_{\partial\Omega_p} F = 0, \quad \oint_{\partial\Omega_d} G = \int_{\Omega_d} J, \quad (1)$$

where  $\Omega_p$  and  $\Omega_d$  are hypersurfaces in the space-time and  $J$  is the source term given by the four-current density. The

electromagnetic variables  $F$  and  $G$  are defined as follows:

$$F = -\sum_{i=1}^3 \mathcal{E}_i dx^0 dx^i + \sum_{j=1}^3 B_j dx^k dx^l \quad (2)$$

$$G = \sum_{i=1}^3 \mathcal{H}_i dx^0 dx^i + \sum_{j=1}^3 D_j dx^k dx^l, \quad (3)$$

where  $\mathcal{E}_i = E_i/c$ ,  $\mathcal{H}_i = H_i/c$ , and  $(j, k, l)$  is a cyclic permutation of  $(1, 2, 3)$ . The constitutive equation relating to  $F$  and  $G$  can be written as

$$F = (Z*)G, \quad (4)$$

where  $Z = \sqrt{\mu/\varepsilon}$  is the impedance of the medium,  $\mu$  and  $\varepsilon$  are the permeability and permittivity, respectively, and  $*$  is the Hodge operator, representing the duality of  $F$  and  $G$ .

For a simple expression of the constitutive equations, the Hodge dual grid [6] is used to satisfy

$$\frac{\int_{S_d} c_r dx^0 dx^j}{\int_{S_p} dx^k dx^l} = -\frac{\int_{S_d} dx^k dx^l}{\int_{S_p} c_r dx^0 dx^j} = \kappa, \quad (5)$$

where  $S_p$  is the face of the primal grid,  $S_d$  is the corresponding face of the dual grid, and  $c_r = 1/\sqrt{\varepsilon_r\mu_r}$  and  $\varepsilon_r$  and  $\mu_r$  are the relative permittivity and permeability, respectively. Condition (5) gives the dual grid that is orthogonal to the primal grid in the Lorentzian metric. Fig. 1 shows an example of a subgrid according to (5) with two divisions in space-time, where the solid line represents the primal grid and the dotted line represents the dual grid. A systematic formulation of the space-time FI method using incidence matrices is presented in [8]. The construction of 4D space-time grid and its resultant computational accuracy is discussed in [9].

## III. CONCEPT OF DEPENDENT DOMAIN

The CFL condition is known as a stability condition for electromagnetic field computation using the FDTD method concept with a brick-type grid. The theory is replaced by the concepts of analytical and numerical dependent domains [5]. The analytical dependent domain  $D_a(t, \tau, x, y)$  and numerical dependent domain  $D_n(t, \tau, x, y)$  are defined as the spatial domains at a given time  $t$  that affect the analytical and numerical

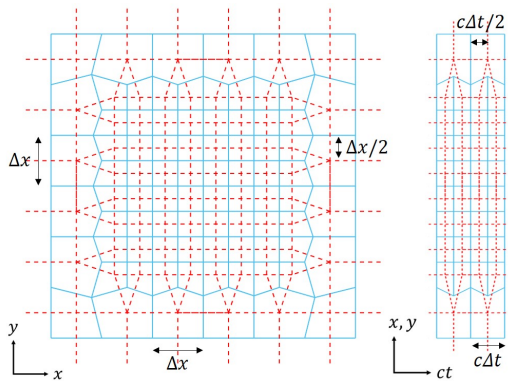


Fig. 1. Subgrid connection; solid line: primal grid, dotted line: dual grid

solutions at time  $\tau > t$  and position  $(x, y)$ , respectively. According to the interpretation of the CFL condition, the numerical propagation speed must exceed the propagation speed of the physical phenomena for numerical stability. In other words, a stable computation is achieved when the numerical dependent domain, which is determined by the propagation of computed information, includes the analytical dependent domain, which is determined by the propagation of the physical phenomena.

By applying this concept to the space-time FI method without a subgrid, the numerical and analytical dependent domains are as illustrated in Fig. 2. The faces, on which the computed information at the space-time point  $(\tau, x, y)$  depend, at time  $t = \tau - \Delta t$ , and  $t = \tau - 2\Delta t$  constitutes the numerical dependent domain. Meanwhile, the analytical dependent domain is the area within the light cone given by the propagation of electromagnetic waves, which is represented by a circle. The inclusion of these domains is considered for all space-time points, and the most critical condition determines the stability limit. This study compares the aforementioned stability criterion with the stability limit obtained by numerical examination for various space-time subgrid geometries.

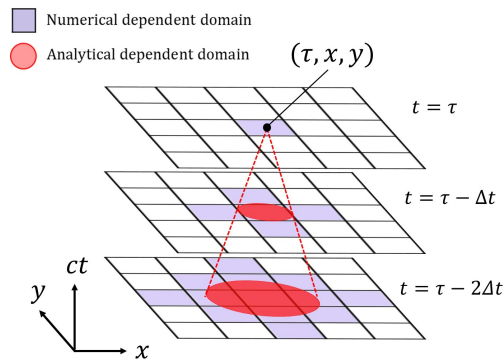


Fig. 2. Dependent domains in 3D space-time

### A. Straight-type 2-Divisions

For the space-time FI method using a subgrid with discrete width  $(\Delta t/2, \Delta x/2(= \Delta y/2))$ , as shown in Fig. 1, we derive

the stability limit from the concept of the dependent domain. Considering the inclusion of numerical and analytical dependent domains at all space-time points, the grid that restricts the stability limit exists at the subgrid boundary, as shown in Fig. 3(a). The computed information at  $(\tau = (n + 1/2)\Delta t, x, y)$  depends on the purple-colored faces at time  $t = n\Delta t$  and  $t = (n - 1/2)\Delta t$ . The numerical dependent domains expand as time goes back. However, at time  $t = (n - 1/2)\Delta t$ , the main grids do not affect the space-time point  $(\tau, x, y)$ , yet; hence, the numerical dependent domain does not expand to the main grid at  $t = (n - 1/2)\Delta t$ . Meanwhile, the analytical dependent domain obtained by the propagation of electromagnetic waves expands regardless of the geometry of the grid. Therefore, the inclusion of the analytical dependent domain with respect to point  $(x, y)$  at  $t = (n - 1/2)\Delta t$  in the numerical dependent domain is achieved by  $c\Delta t \leq d(x', y')$ , as shown in Fig. 3(b), where  $d(x', y')$  is given by

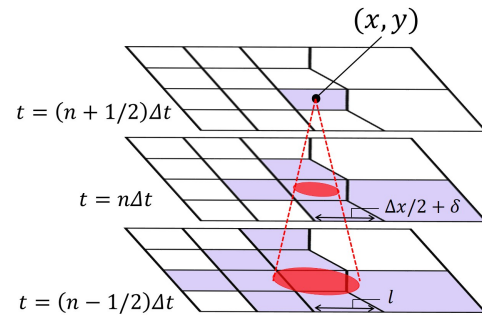
$$d(x', y') = \sqrt{\left(l - \frac{\Delta x}{4}\right)^2 + \left(\frac{\Delta x}{4}\right)^2} \quad (6)$$

$$l = \frac{\Delta x}{2} + \delta + \frac{(c\Delta t)^2}{6\Delta x}. \quad (7)$$

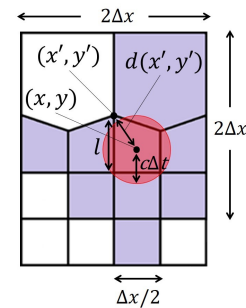
Therein,  $\delta$  is a freeparameter of the grid connection and  $(c\Delta t)^2/6\Delta x$  is due to the slope of the primal face satisfying (5) [Fig. 3]. A grid optimization method [10] gives  $\delta = 0.135\Delta x$ . Therefore, the inclusion condition for the dependent domain is

$$c\Delta t \leq \sqrt{\left[\frac{\Delta x}{4} + \delta + \frac{(c\Delta t)^2}{6\Delta x}\right]^2 + \left(\frac{\Delta x}{4}\right)^2}, \quad (8)$$

which gives the stability limit  $c\Delta t = 0.495\Delta x$ .



(a) Dependent domains at the subgrid boundary in 3D space-time



(b) Dependent domains at  $t = (n - 1/2)\Delta t$

Fig. 3. Dependent domains in space-time subgrid with 2-divisions

### B. Staircase-type 2-Divisions

We set the staircase-type subgrid  $(\Delta t/2, \Delta x/2)$ , as shown in Fig. 4(a); this simplifies the grid connection without changing the nodal positions [7][9]. Considering the dependent domain as in III-A, the stability limit is also restricted by the condition that  $(x, y)$ , shown in Fig. 4(b), at  $\tau = (n + 1/2)\Delta t$  depends on the computed information at  $t = \tau - \Delta t$ ; it is derived by  $c\Delta t \leq d(x', y')$ . Furthermore, because  $d(x', y')$  is determined by the unchanged nodal positions, we obtain exactly the same stability limit  $c\Delta t = 0.495\Delta x$  using (8); therefore, the stability limit is unchanged by the staircase grid connection.

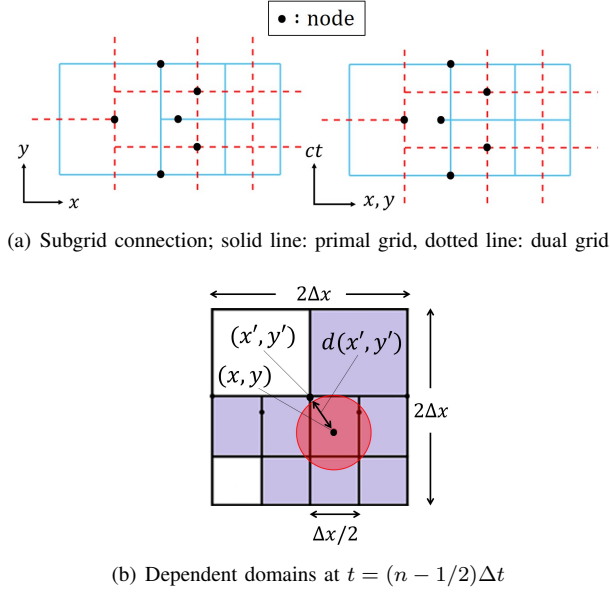


Fig. 4. Subgrid with staircase 2-divisions

### C. Reversed 2-Divisions

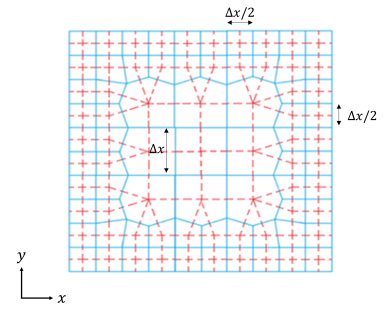
A coarse grid domain is set up inside the subgrid  $(\Delta t/2, \Delta x/2)$  domain; that is, the domains of coarse and fine grids are reversed to the previous setting shown in Fig. 5(a). This arrangement modifies only the corner connections of the subgrid. In this case, the stability limit is restricted by the condition that  $(x, y)$ , as shown in Fig. 5(b), at  $\tau = (n + 1/2)\Delta t$  depends on the computed information at  $t = \tau - \Delta t$ ; it is derived by  $c\Delta t \leq d(x', y')$ , where  $d(x', y')$  is given by

$$d(x', y') = \sqrt{2} \left[ \frac{137\Delta x}{432} + \frac{49(c\Delta t)^2}{432\Delta x} \right]. \quad (9)$$

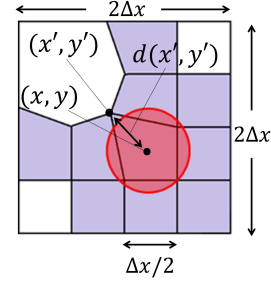
We obtain the stability limit of  $c\Delta t = 0.486\Delta x$ .

### D. 3-Divisions

We discuss the dependent domain when using the subgrid with 3-divisions  $(\Delta t/3, \Delta x/3)$  as shown in Fig. 6. Similar to the case of 2-divisions, the strictest condition in which the numerical dependent domain includes the analytical dependent domain is given by the subgrid boundary connection shown in Fig. 7(a). The inclusion condition of dependent domains at



(a) Subgrid connection; solid line: primal grid, dotted line: dual grid



(b) Dependent domains at  $t = (n - 1/2)\Delta t$

Fig. 5. Subgrid with reversed 2-divisions

$t = \tau - \Delta t$  created by  $(\tau = (n + 1/3)\Delta t, x, y)$  gives  $c\Delta t \leq d(x', y')$ , where  $d(x', y')$  is given by

$$d(x', y') = \sqrt{\left[ \frac{\Delta x}{6} + \delta + \frac{(c\Delta t)^2}{6\Delta x} \right]^2 + \left( \frac{\Delta x}{6} \right)^2} \quad (10)$$

using  $\delta = 0.089\Delta x$ ; thus, we obtain the stability limit  $c\Delta t = 0.314\Delta x$ .

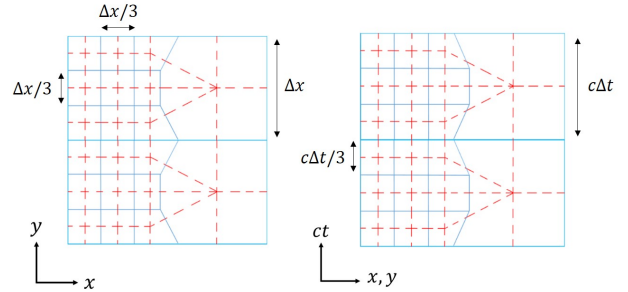


Fig. 6. Subgrid connection with 3-divisions; solid line: primal grid, dotted line: dual grid

### E. 4-Divisions

In the case of a subgrid with 4-divisions  $(\Delta t/4, \Delta x/4)$  [11], the subgrid geometry at the boundary restricts the stability limit according to the concept of the dependent domain. The dependence between  $t = (n + 1/4)\Delta t$  and  $t = (n - 3/4)\Delta t$  at  $(x, y)$  as shown in Fig. 7(b) derives  $c\Delta t \leq d(x', y')$ , where  $d(x', y')$  is given by

$$d(x', y') = \frac{5}{\sqrt{34}} \left[ \frac{\Delta x}{5} + \delta + \frac{3(c\Delta t)^2}{20\Delta x} \right] \quad (11)$$

using  $\delta = 0.089\Delta x$ ; thus, we obtain the stability limit  $c\Delta t = 0.256\Delta x$ .

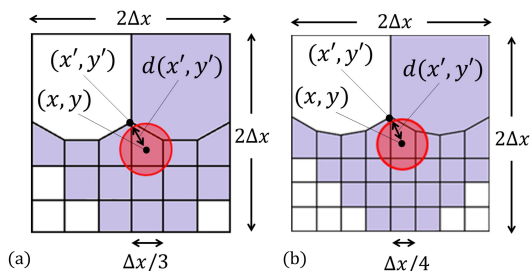


Fig. 7. Dependent domains in space-time subgrid with (a) 3-divisions at  $t = (n - 2/3)\Delta t$  and (b) 4-divisions at  $t = (n - 3/4)\Delta t$ .

#### IV. NUMERICAL EXAMINATION

To evaluate the stability limit based on the concept of the dependent domain, we experimentally obtained the stability limit by numerical examination and compared it with the stability limit due to the dependent domain.

Wave propagation was simulated in the computational domain with the spatially periodic boundary condition, as shown in Fig. 8 with  $c = 1$ ,  $\Delta x = \Delta y = 1$  by normalization and normalized initial conditions given by  $E_x = E_y = E_z = 0$ ,  $B_x = B_y = 0$ , and  $B_z = \exp[-(x^2 + y^2)/25]$ . Fig. 9(a) depicts the distribution of  $B_z$  at  $t = 75\Delta t$  with  $\Delta t = 0.50$  setting the subgrid  $(\Delta t/2, \Delta x/2)$  in Domain I. Meanwhile, Fig. 9(b) describes the distribution of  $B_z$  at  $t = 100\Delta t$  with  $\Delta t = 0.35$  setting the subgrid  $(\Delta t/3, \Delta x/3)$  in Domain II; the wave propagation can also be simulated for the case of the subgrid with 4-divisions.

A long-term computation of 1 million steps is simulated under these conditions, and the upper limit of the time step at which numerical instability does not appear is considered to be the experimentally obtained stability limit. A comparison between the stability limits obtained experimentally and those derived from the concept of a dependent domain is shown in Table I. The stability limits in the cases of straight-type and staircase-type 2-divisions are detailed in [7]; the computational accuracy and non-physical reflections are discussed in [1], [10] and [11]. The results in this table show that the concept of the dependent domain can predict the stability limit of the space-time FI method.

#### V. CONCLUSION

A method for estimating the stability criterion in the 3D space-time FI method based on the concept of the dependent domain is presented. The stability limits given by the concept are consistent with those obtained experimentally by long-term calculations in the cases of the subgrid with straight 2-, staircase 2-, reversed 2-, 3-, and 4-divisions. According to our preliminary experiments, the concept of dependent domain is still valid in the case of 4D space-time subgrid, which will be reported in the future.

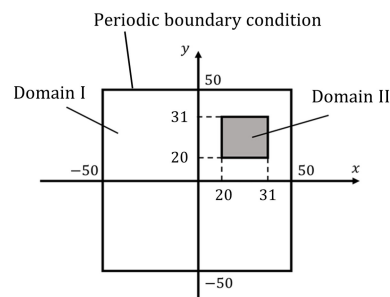


Fig. 8. Computational domain

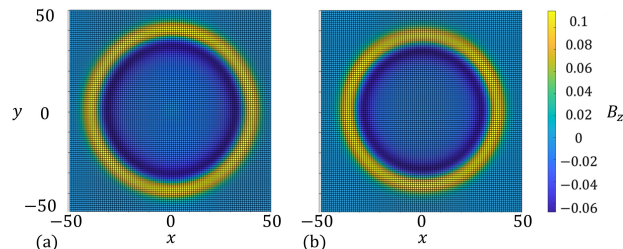


Fig. 9. Wave propagation; (a) reversed 2-divisions and (b) 3-divisions.

TABLE I  
COMPARISON OF STABILITY LIMITS  $c\Delta t/\Delta x$

	Dependent domain	Numerical examination
2-divisions	0.495	0.50 [7]
staircase 2-divisions	0.495	0.50 [7]
reversed 2-divisions	0.486	0.50
3-divisions	0.314	0.35
4-divisions	0.256	0.27

#### REFERENCES

- [1] T. Matsuo, T. Shimoi, J. Kawahara, and T. Mifune, "A simple sub-grid scheme using space-time finite integration method," *IEEE Trans. Magn.*, vol. 51, no. 3, Art. ID 7201904, 2015.
- [2] T. Weiland, "Time domain electromagnetic field computation with finite difference methods," *Int. J. Numer. Model.*, vol. 9, pp. 295-319, 1996.
- [3] I. E. Lager, E. Tonti, A. T. de Hoop, G. Mur and M. Marrone, "Finite formulation and domain-integrated field relations in electromagnetics - a synthesis," *IEEE Trans. Magn.*, vol. 39, no. 3, pp. 1199-1202, 2016.
- [4] P. Thoma and T. Weiland, "A consistent subgridding scheme for the finite difference time domain method," *Int. J. Numer. Model.*, vol. 9, pp. 359-374, 1996.
- [5] J. W. Thomas, *Numerical Partial Differential Equations, Finite Difference Methods*, New York, NY, USA: Springer-Verlag New York, Inc., 1995.
- [6] T. Matsuo, "Space-time finite integration method for electromagnetic field computation," *IEEE Trans. Magn.*, vol. 47, pp. 1530-1533, 2011.
- [7] T. Matsuo, J. Kawahara, T. Shimoi, and T. Mifune, "Stability analysis of space-time finite integration schemes," *COMPEL-Int. J. Comput. Math. Electron. Eng.*, vol. 34, no. 5, pp. 1609-1622, 2015.
- [8] J. Kawahara, T. Mifune, and T. Matsuo, "Geometrical formulation of 3D space-time finite integration method," *IEEE Trans. Magn.*, vol. 49, pp. 1693-1696, 2013.
- [9] K. Arai, T. Mifune, and T. Matsuo, "Space-time PML and subgrid connections for finite integration method," *IEEE Trans. Magn.*, vol. 52, no. 3, 2016.
- [10] Y. Sakata, T. Mifune and T. Matsuo, "Optimal Subgrid Connection for Space-Time Finite Integration Technique," *IEEE Trans. Magn.*, vol. 53, no. 6, 2017.
- [11] Y. Sakata, N. Washio, T. Mifune and T. Matsuo, "Multiple-division subgrid construction for space-time finite integration electromagnetic field computation," *Int. J. Appl. Electromagn. Mech.*, vol. 52, pp. 617-622, 2016.